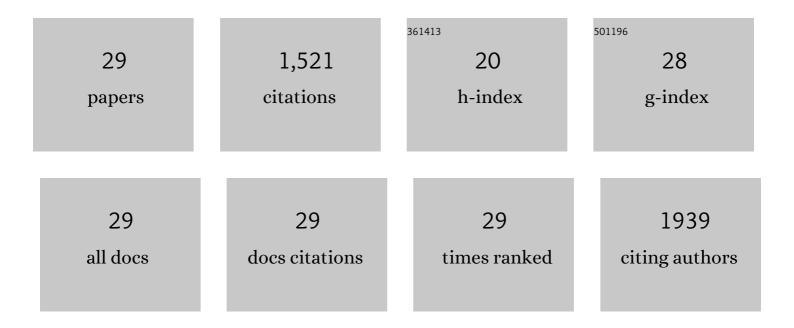
## Zhixiao Qin

List of Publications by Year in descending order

Source: https://exaly.com/author-pdf/10530713/publications.pdf Version: 2024-02-01



ΖΗΙΣΙΛΟ ΟΙΝ

#	Article	IF	CITATIONS
1	CsI Enhanced Buried Interface for Efficient and UVâ€Robust Perovskite Solar Cells. Advanced Energy Materials, 2022, 12, 2103151.	19.5	91
2	Multi‣evel Passivation of MAPbI <sub>3</sub> Perovskite for Efficient and Stable Photovoltaics. Advanced Functional Materials, 2022, 32, .	14.9	36
3	Stable Pure Iodide MA <sub>0.95</sub> Cs <sub>0.05</sub> PbI <sub>3</sub> Perovskite toward Efficient 1.6 eV Bandgap Photovoltaics. Journal of Physical Chemistry Letters, 2022, 13, 5088-5093.	4.6	5
4	Zwitterionâ€Functionalized SnO <sub>2</sub> Substrate Induced Sequential Deposition of Blackâ€Phase FAPbl <sub>3</sub> with Rearranged Pbl <sub>2</sub> Residue. Advanced Materials, 2022, 34, .	21.0	75
5	Decoupling engineering of formamidinium–cesium perovskites for efficient photovoltaics. National Science Review, 2022, 9, .	9.5	22
6	Activating photocatalytic hydrogen generation on inorganic lead-free Cs2AgBiBr6 perovskite via reversible Cu2+/Cu+ redox couple. Journal of Catalysis, 2022, 413, 509-516.	6.2	9
7	Organic Tetrabutylammonium Cation Intercalation to Heal Inorganic CsPbI <sub>3</sub> Perovskite. Angewandte Chemie, 2021, 133, 12459-12463.	2.0	24
8	Organic Tetrabutylammonium Cation Intercalation to Heal Inorganic CsPbI <sub>3</sub> Perovskite. Angewandte Chemie - International Edition, 2021, 60, 12351-12355.	13.8	94
9	Incorporation of Two-Dimensional WSe <sub>2</sub> into MAPbI <sub>3</sub> Perovskite for Efficient and Stable Photovoltaics. Journal of Physical Chemistry Letters, 2021, 12, 6883-6888.	4.6	12
10	Two-Dimensional Materials for Perovskite Solar Cells with Enhanced Efficiency and Stability. , 2021, 3, 1402-1416.		21
11	The ClO· generation and chlorate suppression in photoelectrochemical reactive chlorine species systems on BiVO4 photoanodes. Applied Catalysis B: Environmental, 2021, 296, 120387.	20.2	24
12	Lead Stabilization and lodine Recycling of Lead Halide Perovskite Solar Cells. ACS Sustainable Chemistry and Engineering, 2021, 9, 16519-16525.	6.7	19
13	Synergistic effect of quantum confinement and site-selective doping in polymeric carbon nitride towards overall water splitting. Applied Catalysis B: Environmental, 2020, 261, 118211.	20.2	64
14	Red Phosphorus/Carbon Nitride van der Waals Heterostructure for Photocatalytic Pure Water Splitting under Wide-Spectrum Light Irradiation. ACS Sustainable Chemistry and Engineering, 2020, 8, 13459-13466.	6.7	46
15	Integrated Zâ€Scheme Nanosystem Based on Metal Sulfide Nanorods for Efficient Photocatalytic Pure Water Splitting. ChemSusChem, 2020, 13, 6528-6533.	6.8	17
16	Novel Cu3P/g-C3N4 p-n heterojunction photocatalysts for solar hydrogen generation. Science China Materials, 2018, 61, 861-868.	6.3	84
17	Size- and composition-dependent photocatalytic hydrogen production over colloidal Cd1-xZnxSe nanocrystals. International Journal of Hydrogen Energy, 2018, 43, 13911-13920.	7.1	9
18	Facet‧elective Growth of Cadmium Sulfide Nanorods on Zinc Oxide Microrods: Intergrowth Effect for Improved Photocatalytic Performance. ChemCatChem, 2018, 10, 153-158.	3.7	21

ZHIXIAO QIN

#	Article	IF	CITATIONS
19	Electron-transfer dependent photocatalytic hydrogen generation over cross-linked CdSe/TiO <sub>2</sub> type-ll heterostructure. Nanotechnology, 2017, 28, 084002.	2.6	33
20	Spatial charge separation of one-dimensional Ni2P-Cd0.9Zn0.1S/g-C3N4 heterostructure for high-quantum-yield photocatalytic hydrogen production. Applied Catalysis B: Environmental, 2017, 217, 551-559.	20.2	126
21	A bifunctional NiCoP-based core/shell cocatalyst to promote separate photocatalytic hydrogen and oxygen generation over graphitic carbon nitride. Journal of Materials Chemistry A, 2017, 5, 19025-19035.	10.3	151
22	One-step hydrothermal synthesis of (Culn)0.2Zn1.6S2 hollow sub-microspheres for efficient visible-light-driven photocatalytic hydrogen generation. International Journal of Hydrogen Energy, 2016, 41, 1524-1534.	7.1	13
23	One-step hydrothermal synthesis of Zn x Cd 1â°'x S/ZnO heterostructures for efficient photocatalytic hydrogen production. International Journal of Hydrogen Energy, 2016, 41, 15208-15217.	7.1	30
24	General applicability of nanocrystalline Ni <sub>2</sub> P as a noble-metal-free cocatalyst to boost photocatalytic hydrogen generation. Catalysis Science and Technology, 2016, 6, 8212-8221.	4.1	113
25	Optimization of (Cu <sub>2</sub> Sn) <sub>x</sub> Zn <sub>3(1â^'x)</sub> S <sub>3</sub> /CdS pn junction photoelectrodes for solar water reduction. RSC Advances, 2016, 6, 58409-58416.	3.6	14
26	Composition-Dependent Catalytic Activities of Noble-Metal-Free NiS/Ni <sub>3</sub> S <sub>4</sub> for Hydrogen Evolution Reaction. Journal of Physical Chemistry C, 2016, 120, 14581-14589.	3.1	94
27	Facile Fabrication of Sandwich Structured WO <sub>3</sub> Nanoplate Arrays for Efficient Photoelectrochemical Water Splitting. ACS Applied Materials & Interfaces, 2016, 8, 18089-18096.	8.0	142
28	Intergrowth of Cocatalysts with Host Photocatalysts for Improved Solar-to-Hydrogen Conversion. ACS Applied Materials & Interfaces, 2016, 8, 1264-1272.	8.0	65
29	Noble-metal-free Cu <sub>2</sub> S-modified photocatalysts for enhanced photocatalytic hydrogen production by forming nanoscale p–n junction structure. RSC Advances, 2015, 5, 18159-18166.	3.6	67